LARGE EDDY SIMULATION OF A GAS TURBINE COMBUSTION CHAMBER

G. Bulat*, W. P. Jones, A. Marquis**, V. Sanderson* and U. Stopper*****

w.jones@imperial.ac.uk

* Siemens Industrial Turbomachinery Ltd, Waterside South, Lincoln LN5 7FD, UK

** Imperial College London, Exhibition Road, London SW7 2AZ, UK

*** German Aerospace Centre (DLR), Pfaffenwaldring, Stuttgart D-70569, Germany

Abstract

An industrial gas turbine burner operating at a pressure of 3 bar is simulated using the *sgs-pdf* evolution equation approach in conjunction with the Eulerian stochastic field solution method in the context of Large Eddy Simulation. A dynamic version of the Smagorinsky model is adopted for the sub-grid stresses and eight stochastic fields were utilised to characterize the influence of the sub-grid fluctuations. The chemistry was represented by an ARM reduced GRI 3.0 mechanism with 15 reaction steps and 19 species. The results show good agreement with the experimental data in the flame region at different axial locations. The results serve to demonstrate that simulations of complex combustion problems in industrial geometries are achievable.

Introduction

The turbulent premixed flames to be found in industrial gas turbine combustors are difficult to study due to high levels turbulence, fast chemistry and complex geometrical features. Most of these devices operate at high pressure, which adds to the difficulty of obtaining experimental data and accounting for pressure effects in computational models. Large Eddy Simulation (LES) is a powerful and promising modelling technique particularly for highly swirling and unsteady flows. In case of LES of turbulent combustion, account must be taken of the interactions between turbulence and chemical reaction. The main difficulties encountered in achieving this arise from the filtered chemical source terms, which represents the net rate of species formation and consumption through chemical reaction. Since these reactions are highly non-linear, the filtered values of the fields of chemical species mass fraction and temperature are strongly influenced by the sub-grid scale (sgs) fluctuations of the reactants and the temperature. A method of accounting for these is from the joint scalar probability density function (*pdf*) of all the relevant scalar quantities which provides all the necessary information required to evaluate the filtered chemical source terms.

The modelled form of the equation governing the time evolution of the joint *pdf* of the complete set of scalars provides a means of determining all of the time and spatially varying one-point statistics. The chemical source terms appear in closed form in this equation and no further modelling is required, beyond specification of a chemical reaction mechanism. Due to the high dimensionality of the *pdf* evolution equation, a solution only becomes feasible if stochastic methods are applied. Conventionally Lagrangian stochastic particle methods have been adopted for the *pdf* equation in conjunction with an Eulerian formulation for the velocity and pressure fields. Alternatively, Eulerian approaches have been formulated (see [1] and [2]). These methods introduce stochastic fields, which form a system of stochastic partial differential equations having the same one-point moments as the modelled *pdf* evolution equation, e.g. [3]. A main advantage of the latter method is that the solutions give rise to fields that are continuous

and differentiable in space and which are thus free of spatially varying stochastic errors.

Main Objectives

The LES-*pdf* formulation in conjunction with the Eulerian stochastic field solution method has been successfully applied in a range of burning configurations: ignition [4, 5] and auto-ignition [6], [7], non-premixed [8] and premixed regimes [9]. The majority of cases were at atmospheric pressure and in relatively simple geometrical configurations. This paper aims to validate the LES-*pdf* method for an industrial gas turbine burner (Siemens SGT-100), 1 MW thermal power operating at a pressure of 3 bar. Although the geometrical features of the burner were retained, the operating conditions (pressure, temperature and mixture fractions) studied and discussed in this paper differ from those of the burner in SGT-100 gas turbine. The burner,

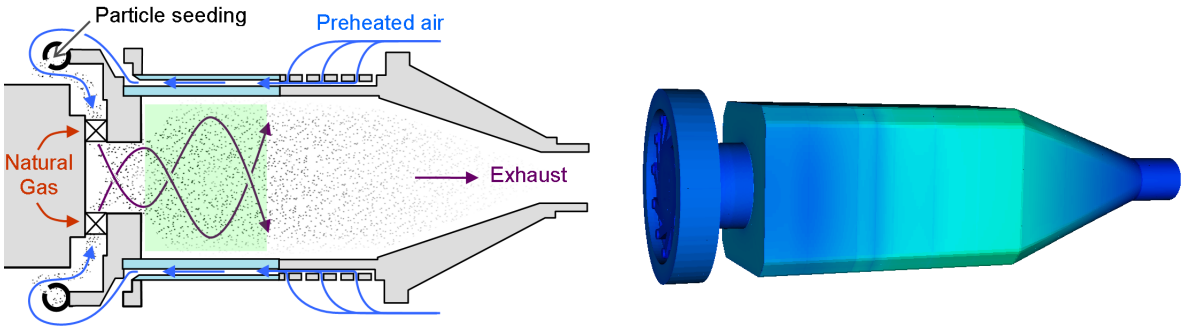

(a) *Experimental setup* (b) *Computational Domain*

Figure 1: Siemens SGT-100 burner, experimental setup and computational domain.

shown in Fig. (1a), was studied experimentally in the high pressure rig facility of the German Aerospace Center (DLR) Stuttgart, Germany [10], [11]. For ease of optical access the combustion chamber was modified so that its cross-section was square. Planar Induced Velocimetry (PIV), 1D Raman and OH PLIF data were collected from the burner. The computational domain used for LES is shown in Fig. (1b)

Large Eddy Simulation

LES involves a direct numerical simulation of the large scale energetic motions with the effects of the unresolved sub-grid scale motions being modelled. The separation of the scales is achieved through a spatial filter, which for a function $f = f(\mathbf{x}, t)$ is defined as its convolution with a filter function G according to:

$$\overline{f}(\mathbf{x}, t) = \int_{\Omega} G(\mathbf{x} - \mathbf{x}'; \Delta(\mathbf{x})) f(\mathbf{x}', t) d\mathbf{x}' \tag{1}$$

The integration is defined over the entire flow domain Ω and the filter function has a characteristic width of Δ, which may vary with position. In combusting flows, strong density fluctuations occur which can be treated through the use of a density weighted filter, defined by $\tilde{f}(\mathbf{x}, t) = \overline{\rho f}/\overline{\rho}$. Applying a density weighted filter to the Continuity and Navier-Stokes equation leads to the following set of filtered equations:

Continuity:

$$\frac{\partial \bar{\rho}}{\partial t} + \frac{\partial \bar{\rho} \tilde{u}_i}{\partial x_i} = 0, \tag{2}$$

Momentum:

$$\frac{\partial \bar{\rho} \tilde{u}_i}{\partial t} + \frac{\partial \bar{\rho} \tilde{u}_i \tilde{u}_j}{\partial x_j} = -\frac{\partial \bar{p}}{\partial x_i} + \frac{\partial}{\partial x_j} \bar{\sigma}_{ij} - \frac{\partial}{\partial x_j} \tau_{ij} \tag{3}$$

where σ_{ij} is the viscous stress tensor and D is the diffusivity, assumed equal for all species and enthalpy. The sub-grid scale stress tensor $\tau_{ij} = \overline{\rho}\left(\widetilde{u_i u_j} - \tilde{u_i}\tilde{u_j}\right)$ is determined via the dynamically calibrated version of the Smagorinsky model proposed by Piomelli and Liu [12]. The filter width Δ is taken as the cubic root of the local grid cell volume.

The filtered forms of the conservation equations for specific molar mass of the chemical species contain the filtered net formation rates of the chemical species through chemical reaction. The direct evaluation of these poses serious difficulties and to overcome these a joint sgs-pdf evolution equation formulation is adopted.

Sub-grid joint *pdf*

An exact equation describing the evolution of the joint sub-grid (or more strictly the filtered fine grained) *pdf* $\widetilde{P}_{\rm sgs}$ can be derived by standard methods, e.g. [13]. This equation contains unknown terms, representing *sgs*-transport of *pdf* and *sgs* micro-mixing. In the present work these are represented, respectively, by a Smagorinsky type gradient model and by the Linear Mean Square Estimation (LMSE) closure, [14]. With these models incorporated the joint —*pdf* equation for the N scalar quantities needed to describe reaction can be written:

$$\begin{aligned} \overline{\rho}\frac{\partial \widetilde{P}_{sgs}(\underline{\psi})}{\partial t} + \overline{\rho}\tilde{u}_j\frac{\partial \widetilde{P}_{sgs}(\underline{\psi})}{\partial x_j} - \sum_{\alpha=1}^{N}\frac{\partial}{\partial \psi_\alpha}\left[\overline{\rho}\dot{\omega}_\alpha(\underline{\psi})\widetilde{P}_{sgs}(\underline{\psi})\right] = \\ +\frac{\partial}{\partial x_i}\left[\left(\left(\frac{\mu}{\sigma}+\frac{\mu_{sgs}}{\sigma_{sgs}}\right)\frac{\partial \tilde{P}_{sgs}(\underline{\psi})}{\partial x_i}\right)\right] - \frac{\overline{\rho}}{\tau_{sgs}}\sum_{\alpha=1}^{N}\frac{\partial}{\partial \psi_\alpha}\left[(\psi_\alpha - \phi_\alpha(\mathbf{x},t))\tilde{P}_{sgs}(\underline{\psi})\right] \end{aligned} \tag{4}$$

where σ_{sgs} is assigned the value 0.7 where $\dot{\omega}_\alpha(\underline{\psi})$ is, in the case of chemical species the net formation rate through chemical reaction. The number of scalar quantities, N is equal to the number of chemical species considered plus one (enthalpy). The micro-mixing time scale is obtained from ${\tau_{sgs}}^{-1} = C_d\frac{\mu+\mu_{sgs}}{\overline{\rho}\Delta^2}$, where $C_d = 2$.

Eulerian stochastic field method

The equation describing the evolution of the *pdf*, equation 4 is solved using the Eulerian stochastic field method. $\tilde{P}_{sgs}(\underline{\psi})$ is represented by an ensemble of N_s stochastic fields for each of the N scalars, namely $\xi_\alpha^n(\mathbf{x},t)$ for $1 \le n \le N_s,\ 1 \le \alpha \le N$. In the present work the Ito formulation of the stochastic integral is adopted and the stochastic fields thus evolve according to:

$$\mathrm{d}\xi_\alpha^n = -\tilde{u}_i\frac{\partial \xi_\alpha^n}{\partial x_i}\mathrm{d}t + \frac{\partial}{\partial x_i}\left[\Gamma'\frac{\partial \xi_\alpha^n}{\partial x_i}\right]\mathrm{d}t + \left(2\Gamma'\right)^{1/2}\frac{\partial \xi_\alpha^n}{\partial x_i}\mathrm{d}W_i^n - \frac{1}{2\tau_{sgs}}\left(\xi_\alpha^n - \tilde{\phi}_\alpha\right)\mathrm{d}t + \dot{\omega}_\alpha^n(\underline{\xi}^n)\mathrm{d}t\ , \tag{5}$$

where Γ' represents the total diffusion coefficient and dW_i^n represent increments of a (vector) Wiener process, different for each field but independent of the spatial location $\mathbf{x}$. This stochastic term has no influence on the first moments (or mean values) of ξ_α^n. The stochastic fields given by (5) are not to be mistaken with any particular realization of the real field, but rather form an equivalent stochastic system (both sets have the same one-point *pdf*, [3]) smooth over the scale of the filter width.

Computational Details

The SGT-100 Dry Low Emission (DLE) burner operating at 3 bar pressure conditions was selected as a test case. The Siemens DLE technology has been proven in the field over the past 22 years and more than 20 million hours of operational experience has been accumulated. The

block-structured finite volume BOFFIN-LES code has been used for the simulations. It utilises a collocated grid arrangement and second order discretisation schemes are used for all gradients, except for the convective part of the scalar equations for which had a TVD-scheme is applied. Eight stochastic fields have been used to characterize the influence of sub-grid fluctuations, as suggested by [15]. The chemical reactions have been calculated using a GRI 3.0 reduced mechanism, [16] with 15 reaction steps and 19 species. A stiff ODE solver has been used to directly integrate the chemical source term. The 8 million cell structured mesh with 240 block-structured domains was generated using ICEM-CFD. The mesh comprises the radial burner, the combustion chamber and a transition duct into an exhaust pipe. Figure 2 presents the mesh in a region of the flame in a cross sectional plane through the combustor. Figure 3 shows the mesh in a cross sectional plane through the swirler with a zoom in region of two vanes.

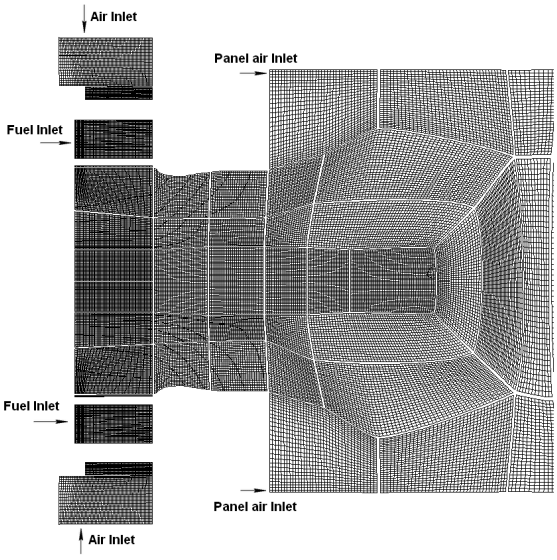

Figure 2: Mesh slices through the combustor with a zoom into the flame region.

The computational domain consists of an air inlet, fuel injection holes, a panel air inlet (experimental leakage) and one outlet. The fuel (German Natural Gas comprising 96.97 % CH_4) with a temperature of 319.8 K was injected through multiple holes inside the swirler vanes. The main combustion air enters the combustor with a temperature of 685.3 K and a bulk velocity of 4.87 m/s. Turbulence is generated in the swirler vanes so steady flow conditions were applied at the inlet boundary. The Reynolds number based on the inlet diameter is 118000. The overall mixture fraction, including the panel air, is 0.0343 (and 0.0374 without the panel air): the stoichiometric value is 0.055. All walls were treated as adiabatic and no radiative heat transfer was included in the calculation. A wall function approach has been used to avoid the need to resolve the flow in the immediate vicinity of the combustor walls.

After passing through the swirler vanes, the flow turns through a right angle into the prechamber, followed by a sudden expansion into the combustion chamber. The geometric swirl number, S_g is 1.3. The flow in the combustion chamber develops into three recirculation regions *(i)* an outer recirculation region formed in the wake of the burner exit and as a result of the combustor square confinement; *(ii)* an inner recirculation region corresponding to the axisymmetric (bubble) vortex breakdown [17] and *(iii)* a weak central recirculation region dominated by the exit confinement. The inner reverse flow zone is attached to the back surface of the burner, thereby establishing a firm aerodynamic base for flame stabilisation. An *M-shaped* flame is stabilized in the shear layers between internal and external flow zones.

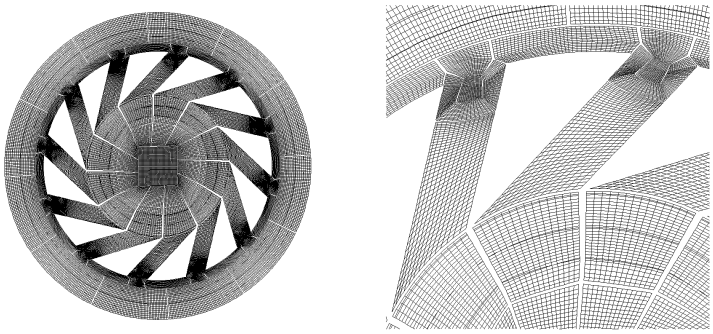

(a) *Swirler Mesh* (b) *Zoom-in of two swirler vanes*

Figure 3: Mesh slices through the swirler with a zoom-in region of two vanes.

Results and Discussions

The main results obtained for the SGT-100 burner are presented and discussed in this section. The simulation has been performed on the Imperial College computer cluster using between 160 and 240 CPU's. The flow field was allowed to settle prior to collection of statistical data. The results of the LES are compared with experimental data at four axial locations ($x/D = 1.21, 1.44, 1.66, 2.00$) as are shown in Figure (4). The time evolution of temperature and species concentrations are studied at selected points in the flame region. The averaged profile of the filtered temperature and filtered CO molar concentration, Figure (4) serves to illustrate the flame position in respect to measurement locations. Also shown are six points at which a detailed analysis of the inner shear region of the flame is provided and where the simulated results are compared with 1D Raman data.

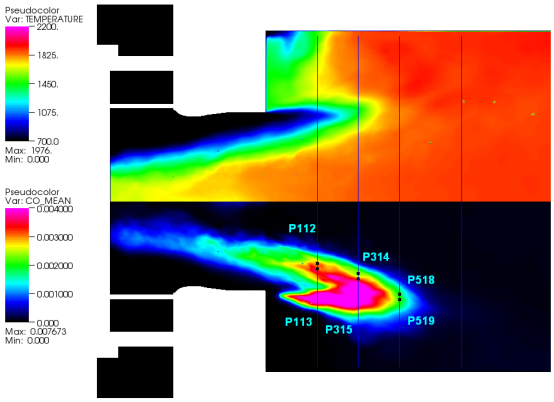

Figure 4: Profiles of mean Temperature and mean CO molar concentration and location of experimental points

The flame index, [18] has been computed as the product of the gradients of methane and oxygen mass fractions and is presented in Figure 5 together with a contour of mixture fraction of 0.0343. The flame index provides a means of distinguishing between premixed and diffusion flame regimes. A positive flame index corresponds to the premixed regime as here the gradients of fuel and oxygen have the same sign whilst negative values corresponds to the diffusion flame

regime. Figure 5 suggests that most of the combustion occurs in a premixed regime, however there are small regions inside the flame where diffusion flame burning exists. It clearly shows that an industrially premixed burner such as SGT-100 has reacting regions of a diffusion nature. This suggests that such a burner operates essentially in the partially premixed regime. The zero (green) region of the flame index signify that there are no interaction between reactants and oxidants, for example in the air inlet region or in the recirculation region where complete combustion has been achieved.

An instantaneous time snapshot of the gradient of the OH molar concentration, the flame index, mixture fraction, temperature, CO and NO molar concentrations in the flame region in the front of the combustor is presented in Figure (5). This shows the complex flame structure captured by the LES-*pdf* model. Regions of local extinction and high local temperature are observed for very similar values of mixture fraction and vortex engulfment of the flame is also captured. Pockets with high values of mixture fraction, corresponding to high temperature values, are captured in fully burned regions (green flame index and small CO concentrations). The finite OH gradients suggest that reaction occurs around these regions, but from the flame index is not clear in which regime combustion occurs. These regions correspond to high concentrations of NO. According to Figure (5), the maximum NO concentration occurs downstream of the flame front whilst the maximum CO concentration occurs in immediate vicinity of the flame front.

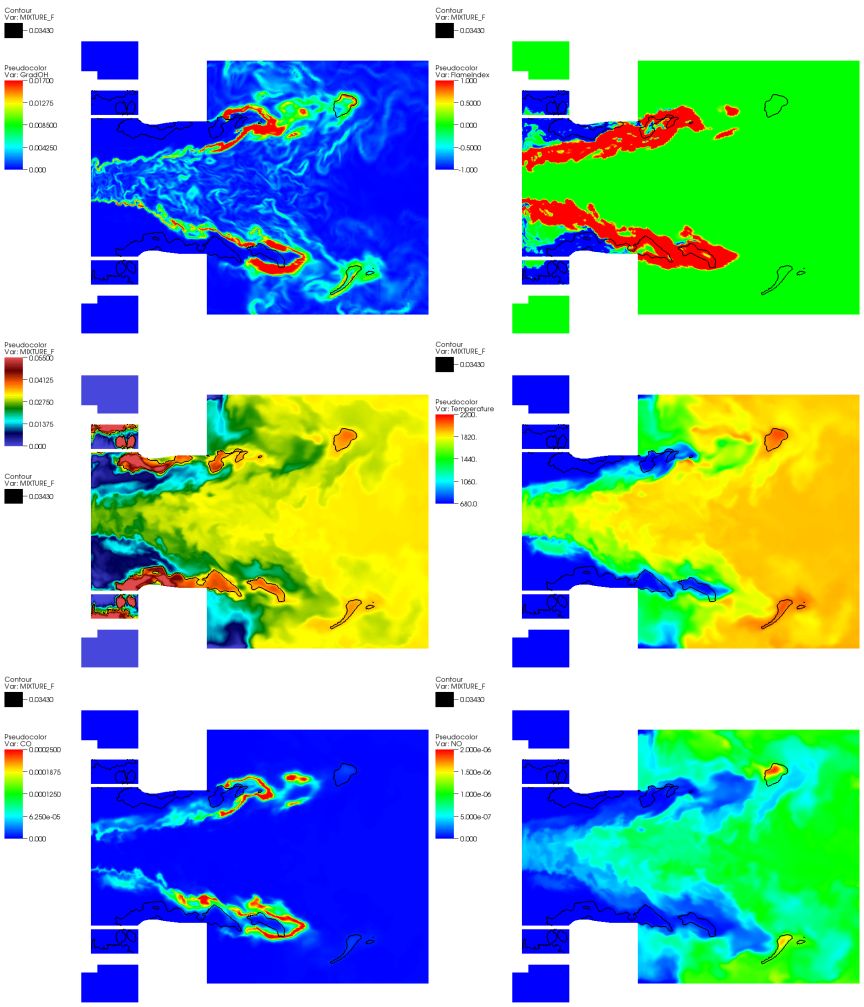

Figure 5: Snapshot of OH Gradient, Flame Index, Mixture Fraction, Temperature CO and NO mole concentration with a contour of the overall burner mixture fraction $f = 0.0343$.

Figure (6) displays a comparison of the simulated and measured (by PIV) mean and RMS axial and radial velocity components at the four different locations shown in Figure (4). The LES simulations reproduce the main flow field well, as can be seen in Figure (6). Both the inner and outer recirculation zones are well captured as are the shear layer regions. The flow field is fully turbulent as is evidenced by the high RMS fluctuations of axial velocity corresponding to approximately 40 % of the mean value. The combustor confinement determines both the size and strength of the inner and outer recirculation zones. On the centre axis a weak region of forward axial flow acceleration, which corresponds to the weak central recirculation region, is observed. This is in agreement with early experimental observations of confined swirling flows [19].

The comparison of mean profiles of temperature, mixture fraction and major species molar concentration is presented in Figures (7) and (8). Mean and RMS temperatures are captured well in the flame regions, however the simulated RMS profiles are too low on the centre axis. Mixing is captured well as confirmed by mixture fraction profiles, Figure (7), however the simulated concentration of methane is low compared with the measurements. This suggests that the fuel, CH_4 is consumed somewhat earlier in the LES than is the case in the experiments.

The time evolution of temperature and species has been collected and compared with the experimental data, [10, 11] at the points indicated in Figure (4). The comparison of the LES results (left) and 1D Raman (mid) measured scatter plots of temperature vs mixture fraction is presented in figure (9). Scaled histograms (to 1000) of mixture fractions are also included for each scatter plot. On the right column the comparison of the simulated and measured (by 1D Raman) *pdf* distributions of temperature are presented for each point. Good agreement is evident at all points within the inner shear layer ($P113$, $P315$). A slight over-estimation of temperature is observed towards the flame tip ($P518$, $P519$). As these points are closer to the combustor wall, it is possible that radiative heat losses (not included in the LES) may have contributed to local quenching in the experiments.

Conclusions

1. A comparison of the flow field simulations with the experimental data shows that the geometry is well resolved and that the use of the dynamic Smagorinsky model is an appropriate sub-grid scale model.

2. The good agreement between the predictions of the temperature and species with the experimental data show that the Eulerian stochastic field method is capable of representing the joint sub-grid *pdf* of the chemical species and the enthalpy.

3. In an industrial premixed burner of this type it is shown that while the majority of the burner operates in the premixed regime small regions exhibit characteristics of diffusion flame burning.

4. The complex geometry, flow, turbulence and combustion of a real industrial burner can be predicted with good accuracy using the LES methodology utilising a sub-grid *pdf* model in conjunction with a stochastic field method.

Acknowledgement

This work was supported by SIEMENS Industrial Turbomachinery Ltd. The support of Dr. Alessio Bonaldo from SIEMENS with processing the experimental data is greatly appreciated.

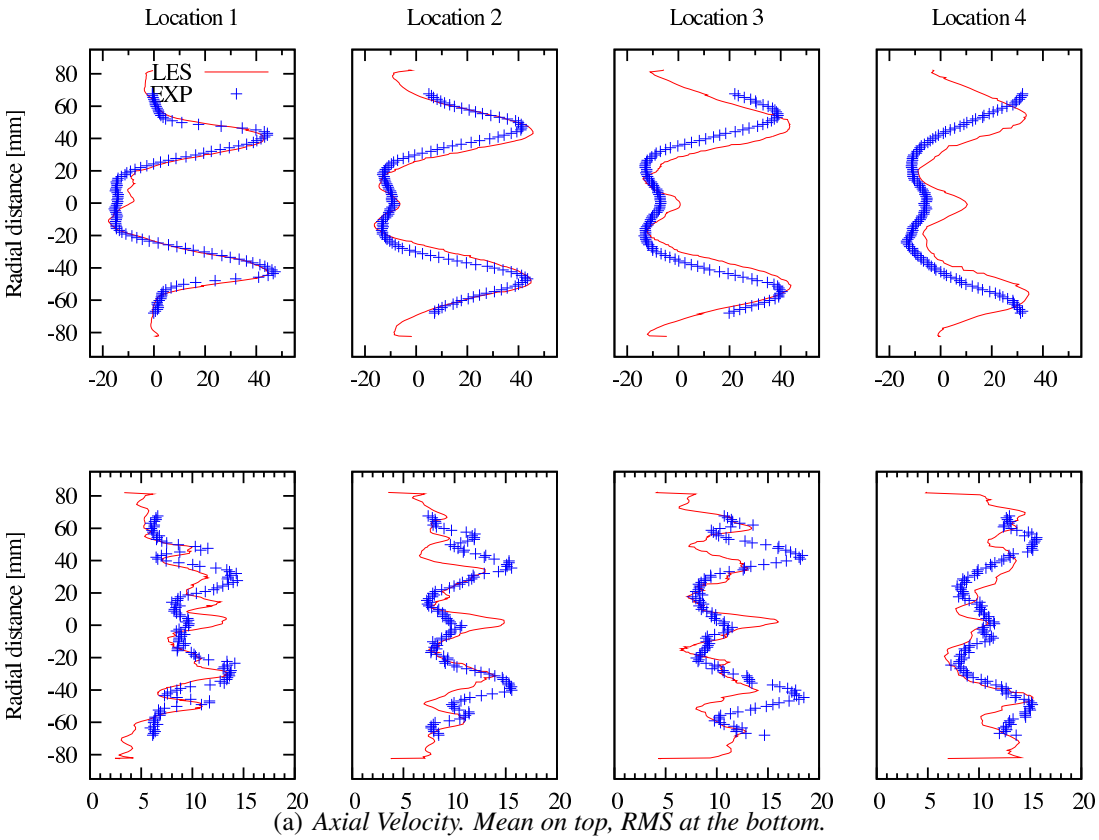

(a) *Axial Velocity. Mean on top, RMS at the bottom.*

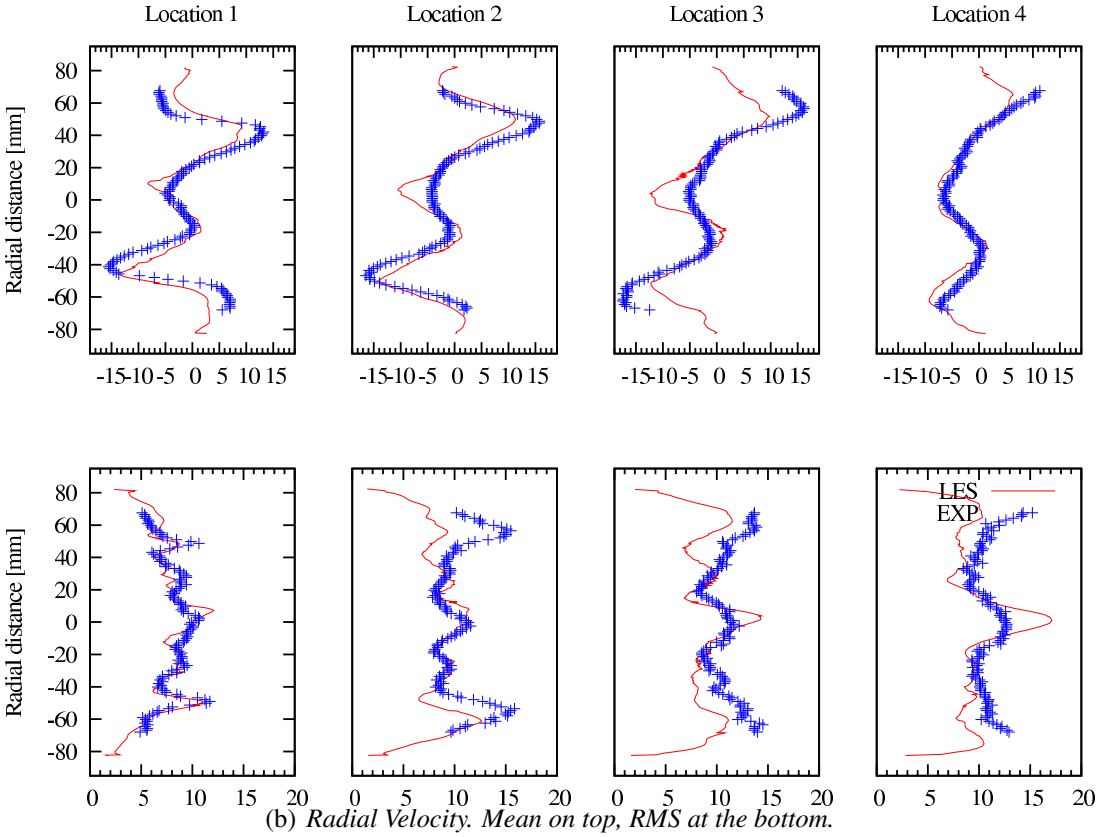

(b) *Radial Velocity. Mean on top, RMS at the bottom.*

Figure 6: Comparison of Axial and Radial Velocity profiles.

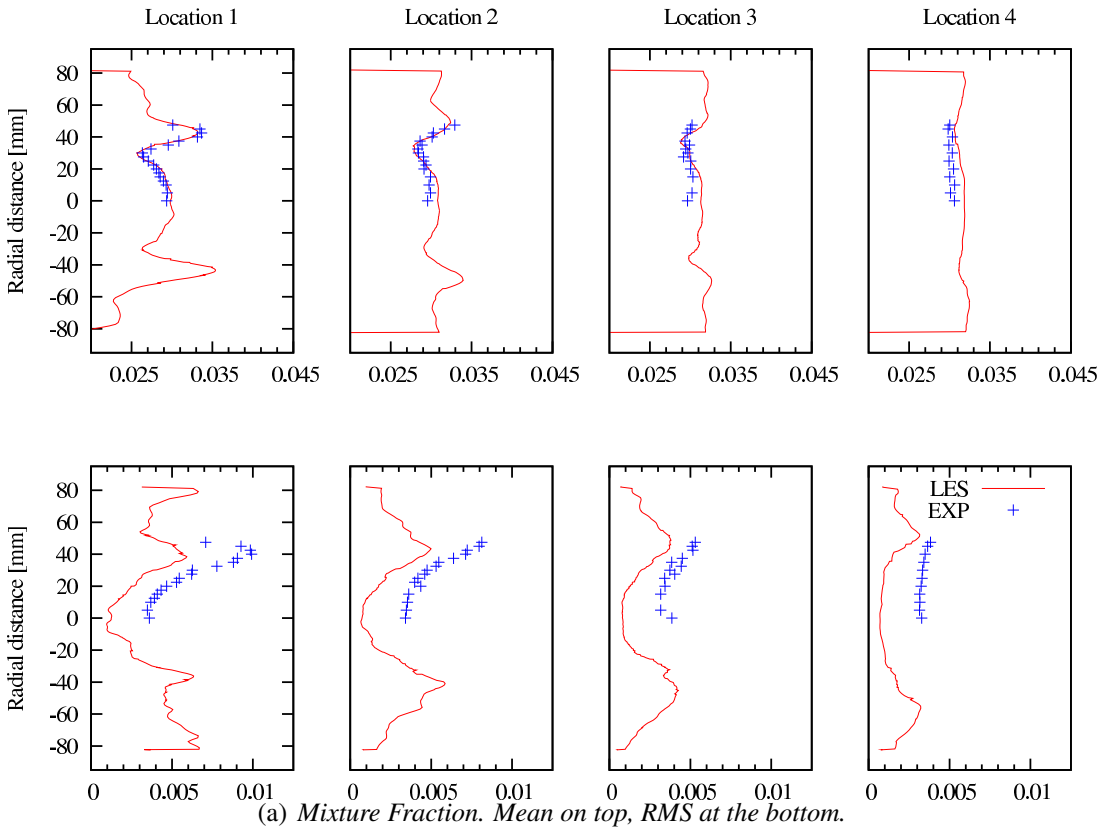

(a) *Mixture Fraction. Mean on top, RMS at the bottom.*

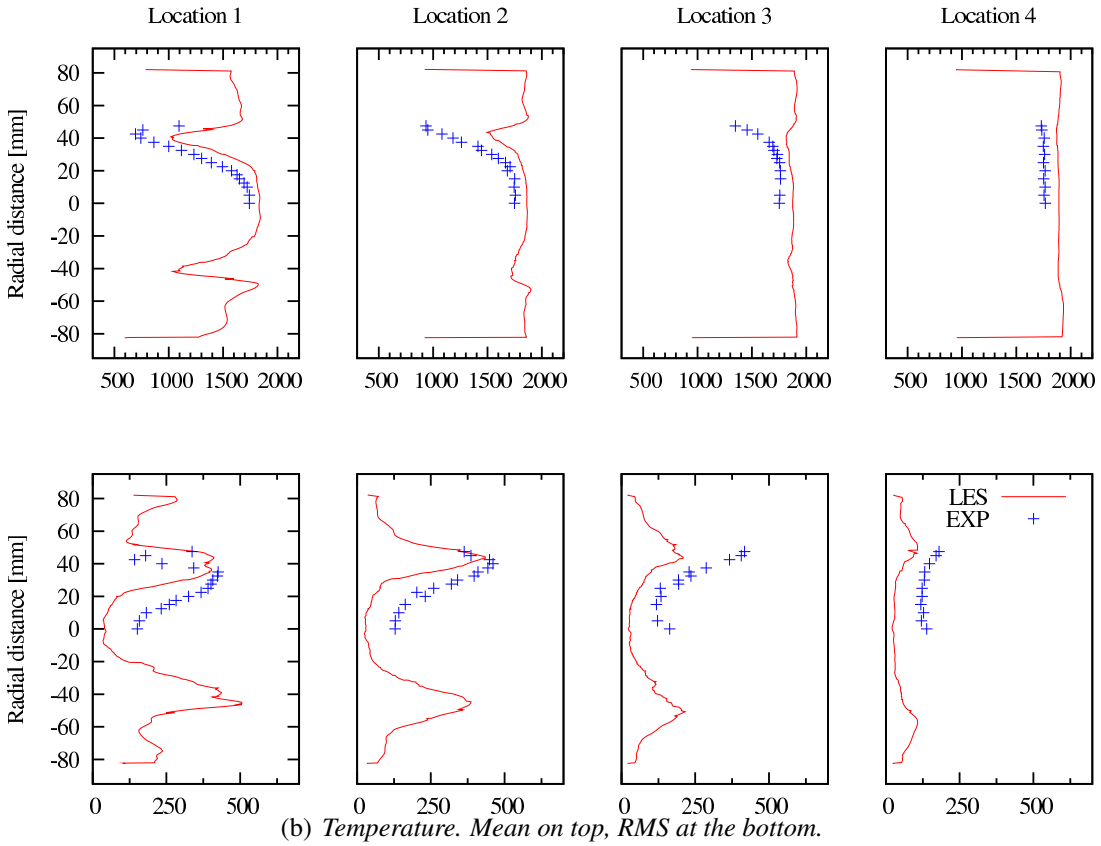

(b) *Temperature. Mean on top, RMS at the bottom.*

Figure 7: Comparison of Temperature and Mixture Fraction profiles.

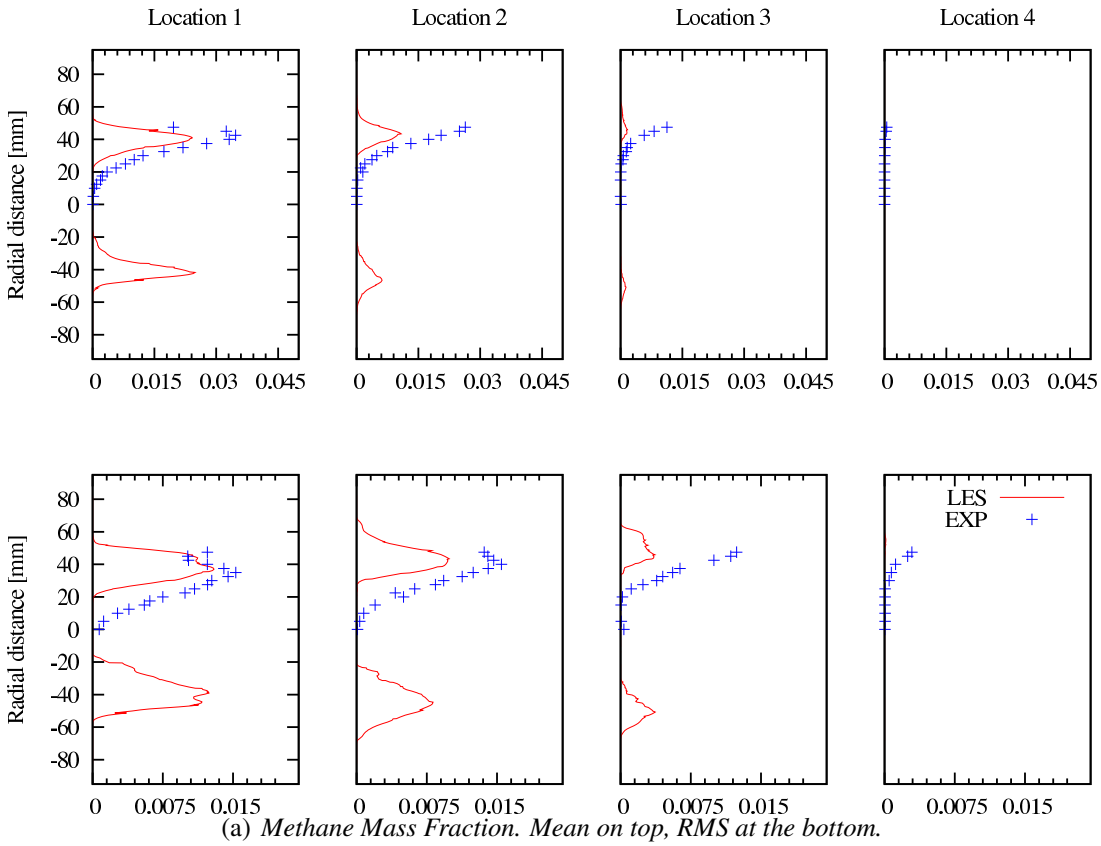

(a) *Methane Mass Fraction. Mean on top, RMS at the bottom.*

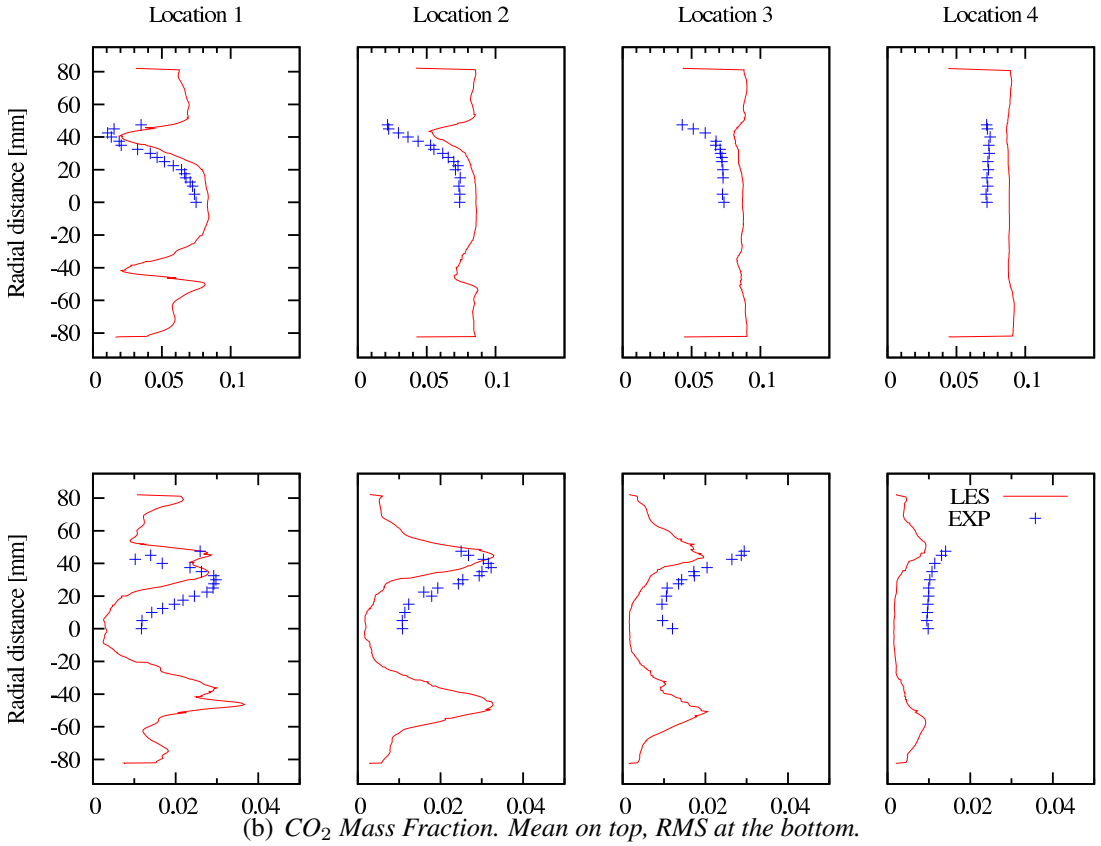

(b) *CO_2 Mass Fraction. Mean on top, RMS at the bottom.*

Figure 8: Comparison of Methane and CO_2 Mass Fraction profiles.

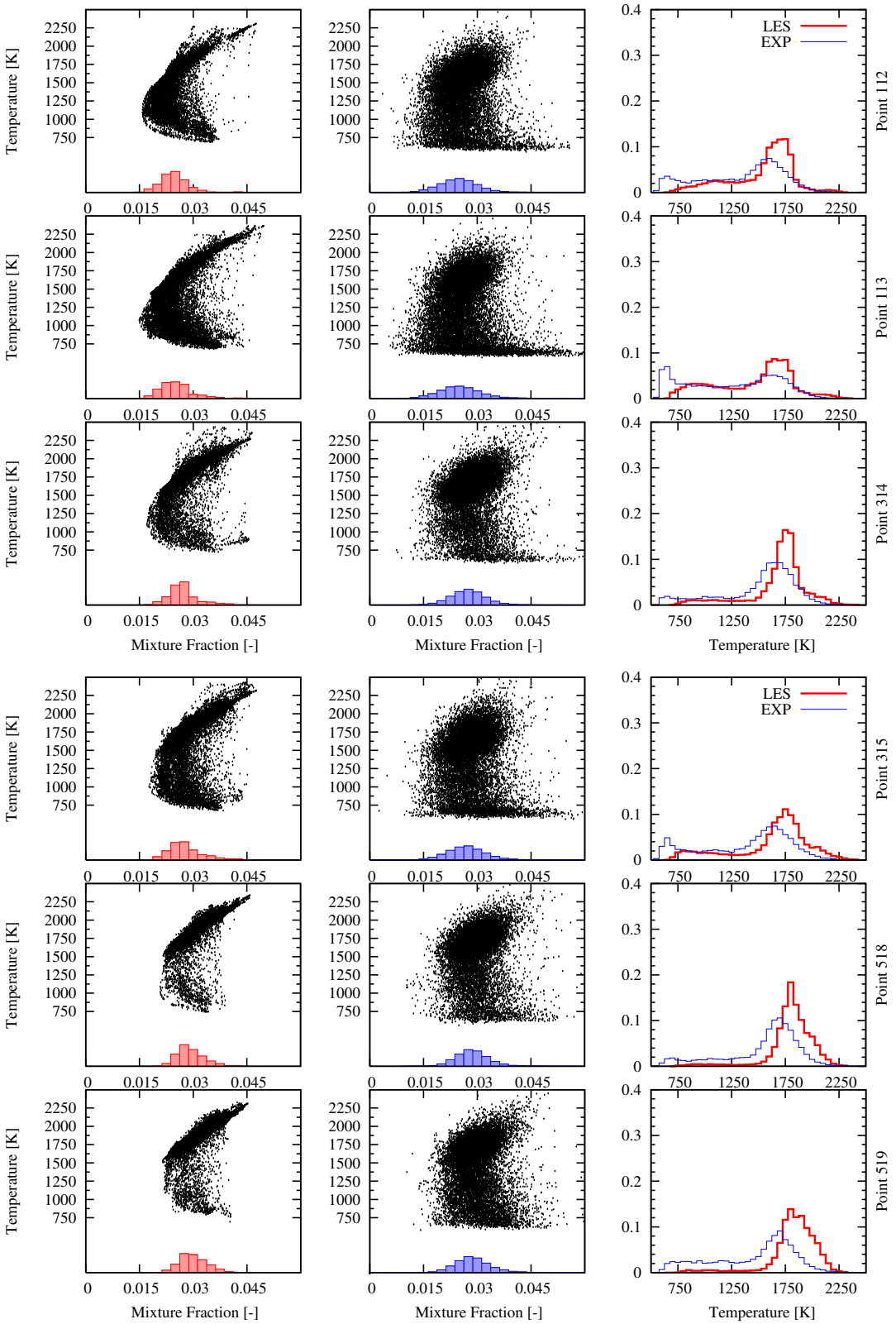

Figure 9: Comparison of Scatter Plots between LES (left) and 1-D Raman (mid) and *pdf* of temperature (right).

References

[1] L. Valino. A field Monte Carlo formulation for calculating the probability density function of a single scalar in a turbulent flow. *Flow, Turbulence and Combustion*, 60(2):157–172, 1998.

[2] V. Sabel'nikov and O. Soulard. Rapidly decorrelating velocity-field model for as a tool for solving one point Fokker-Planck equations for probability density functions of turbulent reactive scalars. *Physial Review E*, 72(1):016301, 2005.

[3] C. Gardiner. *Handbook of Stochastic Methods*. Springer Verlag, 1985.

[4] W. P. Jones and A. Tyliszczak. Large eddy simulation of spark ignition in a gas turbine combustor. *Flow Turbulence Combust.*, 85:711–734, 2010.

[5] W. P. Jones and V. N. Prasad. LES-pdf of a spark ignited turbulent methane jet. *Proceedings of The Combustion Institute*, 2011. in press.

[6] W. P. Jones and S. Navarro-Martinez. Large eddy simulations of autoignition with a subgrid probability density method. *Combustion and Flame*, 150(3):170–187, 2007.

[7] W. P. Jones and S. Navarro-Martinez. Study of hydrogen auto-ignition in a turbulent air co-flow using large eddy simulation approach. *Computers & Fluids*, 37:802–808, 2007.

[8] W. P. Jones and V. N. Prasad. Large eddy simulation of the Sandia flame series (D-F) using the Eulerian stochastic field method. *Combustion and Flame*, 157(9):1621–1636, 2010.

[9] V.N. Prasad. *Large Eddy Simulation of partially premixed turbulent combustion*. PhD thesis, Imperial College, University of London, 2011.

[10] U.Stopper, M. Aigner, W. Meier, R. Sadanandan, M. Stör, and I.S. Kim. Flow field and combustion characterisation of premixed gas turbine flames by planar laser techniques. *Journal of Engineering for Gas Turbines and Power*, 131(2), 2009.

[11] U.Stopper, M. Aigner, H. Ax, W. Meier, R. Sadanandan, M. Stör, and A. Bonaldo. PIV, 2D-LIF, and 1-D raman measurements of flow field, composition and temperature in premixed gas turbine flames. *Experimental Thermal and Fluid Science*, 34(3), 2010.

[12] U. Piomelli and J. Liu. Large eddy simulation of rotating channel flows using a localised dynamic model. *Physics of Fluids*, 7(4):839–848, 1995.

[13] F. Gao and E. O'Brian. A large-eddy simulation scheme for turbulent reacting flows. *Physics of Fluids A*, 5:1282–1284, 1993.

[14] C. Dopazo. Relaxation of initial probability density functions in the turbulent convection of scalar fields. *Physics of Fluids*, 22(1):20–30, 1979.

[15] Radu Mustata, Luis Valiño, Carmen Jimenez, W. P. Jones, and S. Bondi. A probability density function Eularian Monte-Carlo field method for large eddy simulations: Application to a turbulent piloted methane/air diffusion flame (sandia d). *Combustion and Flame*, 145:88–104, 2006.

[16] C. J. Sung, C. K. Law, and J. Y. Chen. Augmented reduced mechanisms for no emission in methane oxidation. *Combustion and Flame*, 125(906-919), 2001.

[17] T. Sarpkaya. On stationary and travelling vortex breakdowns. *Journal of Fluid Mechanics*, 45(3):545–559, 1971.

[18] Y. Mizobuchi, S. Tachibana, J. Shinio, S. Ogawa, and T. Takeno. A numerical analysis of the structure of a turbulent hydrogen jet lifted flame. *Proceedings of The Combustion Institute*, 29(1):2009–2015, 2002.

[19] N. Syred and J. M. Beér. Combustion in swirling flows: a review. *Combustion and Flame*, 23:143–201, 1974.